

# Photoluminescence characterization of Si-based nanostructured films produced by pulsed laser ablation

A. V. Kabashin<sup>a)</sup> and M. Meunier

*Département de Génie Physique, Ecole Polytechnique de Montréal, Case Postale 6079, succ. Centre-ville, Montréal, Québec H3C 3A7, Canada*

R. Leonelli

*Département de Physique, Université de Montréal, C.P. 6128, succ. Centre-ville, Montréal, Québec H3C 3J7, Canada*

(Received 14 September 2000; accepted 1 October 2001)

Photoluminescence (PL) properties of nanostructured Si-based films produced by pulsed laser ablation in a residual gas are studied. Two types of PL signals have been identified. Signals of the first type are sensitive to the ablation conditions with the PL peak position depending on the gas pressure during the deposition. Signals of the second type with PL peaks around 1.6–1.7 and 2.2–2.3 eV are almost independent of the ablation conditions and are mainly determined by the presence of oxygen-related complexes in the film composition. These complexes can be formed through a prolonged natural oxidation or thermal annealing of the films, or through the direct laser ablation in the presence of oxygen. Possible mechanisms of PL signals are discussed. © 2001 American Vacuum Society. [DOI: 10.1116/1.1420494]

## I. INTRODUCTION

Silicon is a leading semiconductor in the modern microelectronics industry. However, its indirect and small (1.11 eV at room temperature) band gap has complicated the spreading of Si-based technologies to optoelectronics for a long time. Recent observations of visible photoluminescence (PL) at room temperature from porous silicon<sup>1</sup> and nanostructured Si-based films fabricated by various methods, such as, for example, magnetron sputtering,<sup>2</sup> laser breakdown in silane,<sup>3</sup> plasma-enhanced chemical vapor deposition,<sup>4</sup> ion implantation,<sup>5</sup> etc., enable one to reexamine the optoelectronics application of silicon-contained materials and give a promise for the creation of silicon-based optoelectronics devices.

Pulsed laser ablation (PLA) is one of the “dry” techniques, which could be especially interesting for the fabrication of Si-based devices due to a good compatibility with silicon processing technology. PLA makes possible a fine variation of the nanocluster parameters during the deposition<sup>6–9</sup> and a formation of Si/SiO<sub>x</sub> films containing silicon nanocrystallites (see, e.g., Refs. 10–17). However, PL properties from laser-ablated films were not similar in different studies. Some groups reported nearly fixed PL peaks for the films deposited in different conditions,<sup>11–15</sup> whereas other teams observed a clear shift of the PL peak when the particle size was changed by a variation of deposition parameters.<sup>16</sup> In our opinion, such a difference in PL properties may be connected to not only different ablation parameters, but to different postdeposition conditions as well. For example, in some studies<sup>12–15</sup> the films were thermally annealed after the fabrication, that could additionally modify their properties. We believe that to get a better understanding of the PL origin, one must clearly separate the contribution from the laser

ablation itself and from the postdeposition conditions.

In this article, we compare PL properties of as-deposited and postoxidized films and thus identify PL peaks related to different phenomena. The main attention is given to the visible and near-infrared ranges of the spectrum (*S* band), which are the most important for optoelectronics applications.

## II. EXPERIMENTAL SETUP

The ablation of material from a rotating Si target [(1-0-0), *N*-type, resistivity 10 Ω cm] was produced by a pulsed KrF laser ( $\lambda=248$  nm, pulse length 15 ns full width at half maximum, repetition rate 30 Hz). The radiation was focused on a focal spot  $2\times 1$  mm<sup>2</sup> on the target at the incident angle of 45°. The fluence was 7–10 J/cm<sup>2</sup> giving a radiation intensity of about  $5\times 10^8$  W/cm<sup>2</sup>. The laser-induced plasma plume expanded perpendicularly to the target surface. The substrates, identical to the target, were placed on a rotating substrate holder 2 cm from the target. Both the target and the substrate were kept at room temperature. The deposition was carried out in He (purity 99.9995%) at a constant ambient pressure. The pressure *P* of He was varied in different experiments between 50 mTorr and 10 Torr, while the laser pulse energy and target-to-substrate distance were fixed. The chamber was pumped down to  $P=2\times 10^{-7}$  Torr before filling with the gas. Under the residual air pressure of  $2\times 10^{-7}$  Torr and the laser repetition rate of 30 Hz, oxidation of ablated silicon layers is negligible between the laser pulses.<sup>16</sup> After several thousand laser shots, the thickness of the Si film on the substrate was 100–1000 nm. For some comparative tests the deposition was also performed in pure oxygen. The pressure of oxygen did not exceed 200 mTorr in order to maintain a relatively intense plasma plume.

In addition, a technique of thermal evaporation from a Si target in vacuum has been used for comparative tests. In contrast to PLA, this technique is known to provide amor-

<sup>a)</sup>Electronic mail: akabach@email.phys.polymtl.ca

phous films with relatively large dimensions of deposited particles. Powder from a Si wafer with the same parameters was evaporated under the residual pressure of  $10^{-7}$  Torr from a tantalum boat onto a Si substrate maintained at room temperature. The boat to substrate distance was about 15 cm, and the deposition rate was 0.1 to 0.2 nm/s as measured by a quartz microbalance system. The thickness of deposited amorphous Si films on the substrate was 100–200 nm. To estimate the PL efficiency from the films fabricated by PLA we also prepared samples of porous silicon by an anodization etching of a Si wafer, identical to the PLA target, in a 1:1 mixture of 49% HF and ethanol. The anodizing current of 30 mA/cm<sup>2</sup> and the etching time of 5–20 min were selected to provide maximal PL intensity of the porous silicon samples. In some cases, the films deposited by PLA and thermal evaporation were annealed at 800 °C in atmospheric air for 10 min. The increase and decrease rates of temperature were 10 °C/min.

For the PL measurements the samples were illuminated by the radiation of a cw Ar<sup>+</sup> laser (model INNOVA 100) with the wavelength 488 nm. The power was 10 mW and the power density on the analyzed samples was estimated to be 30 W/cm<sup>2</sup>. The PL spectra were measured at room temperature using a double spectrometer (model U100, Instruments SA) and GaAs photomultiplier (Hamamatsu Photonics). The spectra were corrected to take into account the spectral response of the PL setup.

The x-ray diffraction spectroscopy (XRD) technique was used to examine structural properties of the films and estimate minimal dimensions of particles in the deposit. To determine the composition of the surface layer, the films were also analyzed by x-ray photoemission spectroscopy (XPS) at a base pressure of  $2 \times 10^{-8}$  Torr using a Thermo VG Scientific system.

### III. RESULTS

The laser-ablated thin films were colored. While deposited under relatively low He pressures between 0.2 and 1 Torr, the films manifested distinct multicolor interference fringes due to the nonuniform film thickness. However, the fringes were absent for He pressures higher than 1.5–2 Torr. In this case the films were yellow or yellow-gray deposits. The disappearance of interference fringes was probably connected to a granular, porous-like microstructure of the deposit, which prevented the interference in reflected white light.

XRD spectra of the films are shown in Fig. 1(a). One can see that the spectra exhibited all peaks typical for crystalline silicon. These peaks could be clearly identified for all samples fabricated under different helium pressures. It is worth mentioning that XRD spectra of some samples deposited at reduced pressures  $P=0.2\text{--}0.3$  Torr could also contain a minor amorphous fraction. It is known<sup>18</sup> that the broadness of XRD peaks is mainly determined by clusters of the smallest crystals in the deposit. As the instrumental noises are relatively low, this property could be used to estimate with a fair accuracy (see, e.g., Ref. 19) the minimal size of crystals in the deposit by the Debye–Scherrer formula.<sup>18</sup>

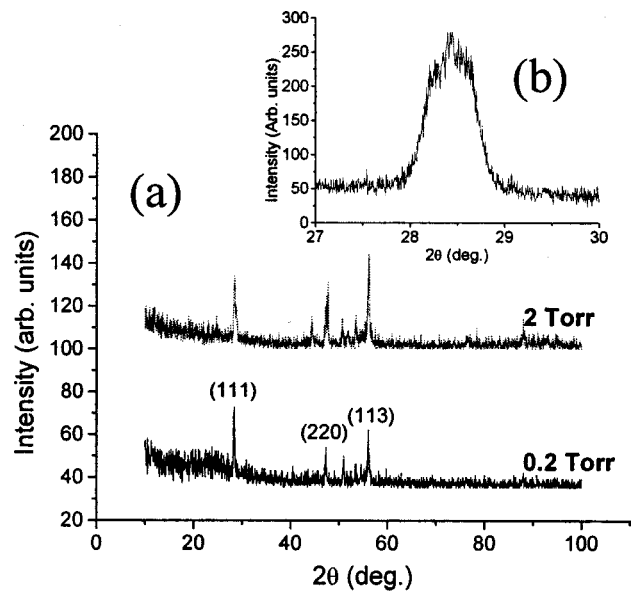


FIG. 1. (a) Typical x-ray diffraction spectra from Si-based films prepared by laser ablation under different helium pressures. (b) Highly resolved XRD spectrum near a crystalline silicon line for the film deposited under 2 Torr of helium.

Taking the broadness of a typical silicon peak [ $\Delta(2\theta)/2 = 0.65^\circ$ ] from a highly resolved XRD spectrum [Fig. 1(b)], the estimation gives the minimal grain size of about 10 nm, which is in good agreement with the average particle size values estimated from transmission electron microscopy (4–10 nm)<sup>11,12</sup> and atomic force microscopy (1–10 nm)<sup>13,16,20</sup> images of laser-ablated silicon deposits.

The surface composition of the films was examined by x-ray photoelectron spectroscopy (XPS). Figure 2 shows the XPS spectra of a film just after its fabrication (spectrum 1) and after 8 weeks of its exposure to ambient air (spectrum 2). The spectrum of the as-deposited sample (1) demonstrates two peaks at about 99.8 and 103.2 eV, which are assigned to the Si 2p photoelectrons of the unoxidized Si core and the

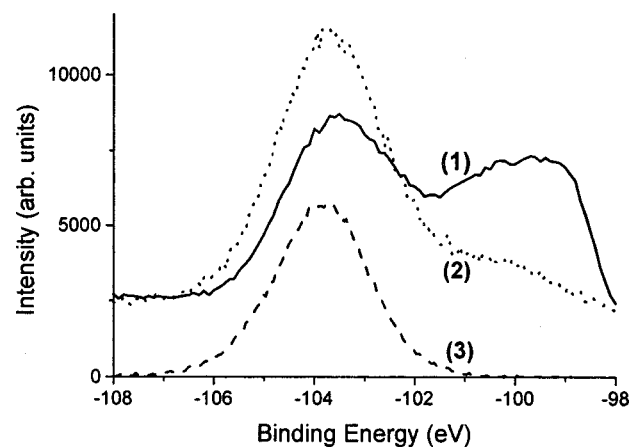


FIG. 2. Typical XPS spectra from the films prepared by laser ablation under 2 Torr of helium just after their fabrication (1) and after 10 weeks of exposure to ambient air (2). (3) Typical XPS spectrum of the film deposited under 0.15 Torr of oxygen.

SiO<sub>x</sub> oxide layer, respectively. The spectrum of the oxidized sample (2) reveals a decrease of the low-energy peak with a slight shift to higher binding energies. On the other hand, the high-energy peak becomes stronger and shifts to higher energies up to 104 eV, which is assigned to 2*p* photoelectrons of pure SiO<sub>2</sub>. Our XPS results shown in Fig. 2 agree well with those of previous studies of SiO<sub>x</sub> films (see, e.g., Ref. 21). The change of the spectrum observed by increasing the oxidation time correlates fairly well with that observed by increasing *x*.<sup>21</sup> It means that the composition *x* of the surface oxide increases as the exposure time increases. For the comparison, the films deposited in pure oxygen were also analyzed by XPS. In this case we only observed the peak at about 104 eV (spectrum 3), which corresponds to the photoelectrons of pure SiO<sub>2</sub>. Similar spectra were observed after the thermal annealing of the films deposited in helium, suggesting that the annealing led to a profound film oxidation.

For the PLA in He ambient, PL signals from the films were observed only after the exposition of the films to oxygen, i.e., after the replacement of He in a vacuum chamber by atmospheric air. It was controlled *in situ* with a naked eye and an integral Si photodetector just after the deposition process. For this purpose the films were irradiated by a cw Ar<sup>+</sup> laser with the intensity of 30 W/cm<sup>2</sup>, while an optical filter was cutting the main laser radiation.

Measurements of PL spectra were performed just after the film exposition to ambient air. They revealed relatively weak PL signals with the peak position depending on the helium pressure during the deposition. In particular, the decrease of the He pressure from 2 Torr to 150 mTorr in different deposition experiments caused a progressive shift of the PL peak position from 1.6 to 2.10–2.12 eV as shown in Fig. 3(a). However, a wider displacement of the PL peak position by this method was not possible. Under the pressures above 2 Torr, PL peaks remained always around 1.6–1.7 eV, while their intensity decreased significantly. On the other hand, the decrease of the pressure below 150 mTorr caused a dramatic decrease of the plasma plume intensity, which led to too weak and hardly reproducible PL signals. Nevertheless, maximum PL intensities were found to be remarkably different for the peaks within the 1.6–2.15 eV range. The most intense PL signals were at about 1.60–1.65 eV, while PL intensities of other peaks could be weaker by orders of magnitude as shown in Fig. 3(b). Thus in our experimental conditions there was a narrow pressure optimum around 1.5–3 Torr, which made possible the production of Si-based films with relatively strong PL. The maximal signals were very strong and easily visible by a naked eye, but they were weaker by a factor of 40–60 than the maximal PL signals from a porous silicon sample produced by anodization etching. It should be noted that the porous silicon layers were much thicker (5–10 μm) than the laser-ablated films (0.1–1 μm).

Our experiments showed that oxidation phenomena could cause a dramatic change of the PL properties of laser-ablated films. In particular, the films deposited under relatively high helium pressure  $P > 1.5$  Torr suffered considerable modifica-

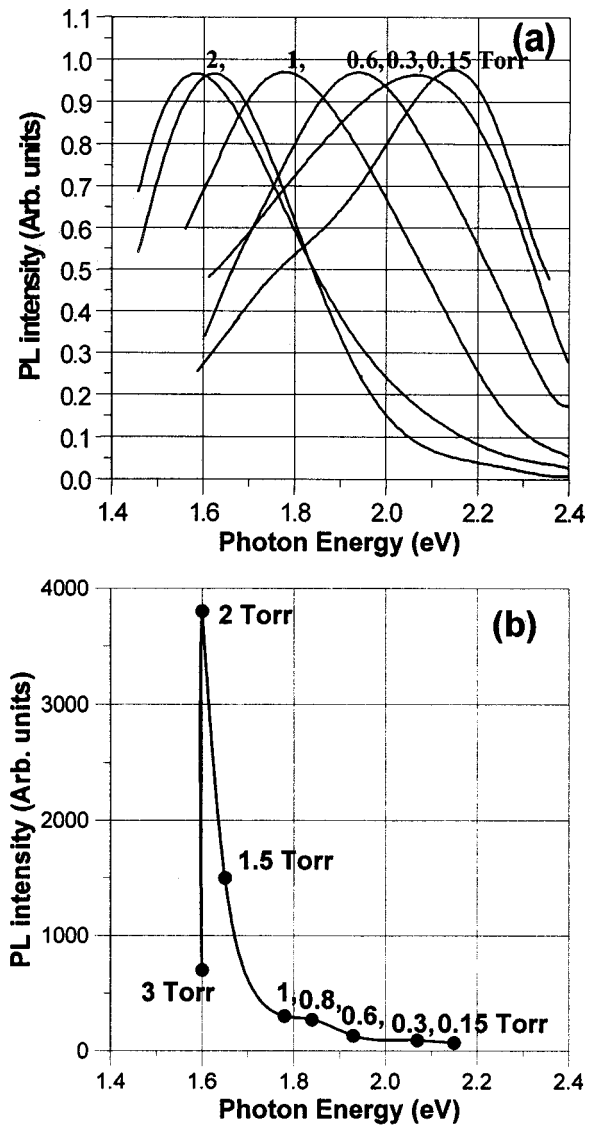


FIG. 3. (a) Photoluminescence spectra of Si/SiO<sub>x</sub> films deposited at different He pressures. Spectra intensities are normalized to the peak value. (b) Integral PL intensities for spectra with different peaks.

tion of PL spectra under a prolonged natural oxidation of the films in atmospheric air. Just after the fabrication, these films exhibited PL signals with the peak energy at about 1.6–1.7 eV. However, the prolonged film exposition to air led to a considerable enhancement of the intensity of these signals, as shown in Fig. 4. The PL integral intensity could increase by a factor of 4–10 and stabilized only after 8–10 weeks. The intensity enhancement was accompanied by a slight redshift of the PL peak intensity by about 0.03–0.05 eV. A set of special tests showed that the increase rate of 1.6–1.7 eV signals could be accelerated by an increase of the air relative humidity. In addition, a prolonged storage of samples fabricated under  $P > 1.5$  Torr in a relatively humid atmosphere could lead to the appearance of another PL peak at about 2.2–2.3 eV as shown in Fig. 5 [spectrum (He)]. The enhancement of fixed 1.6–1.7 and 2.2–2.3 eV components under the prolonged film exposition to air correlated well with

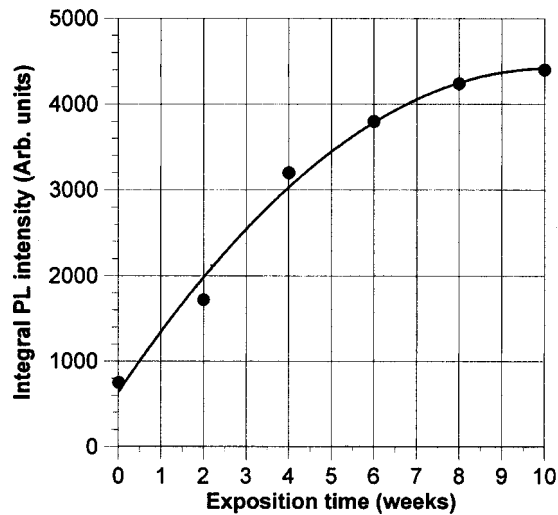


FIG. 4. Integral PL intensity for 1.6 to 1.7 eV signals as a function of exposition time. The film was deposited in He at  $P=2$  Torr.

the relative increase of  $x$  in oxygen-related  $\text{SiO}_x$  complexes ( $0 < x < 2$ ) of the upper film layer, as measured by XPS (see Fig. 2). Such correlation between spectral and surface composition modifications gives evidence for the oxidation-related origin of these components.

Note that the films deposited under reduced helium pressures  $P < 1$  Torr did not demonstrate any spectral modifications under a prolonged natural oxidation of the films. In our opinion, such a difference between PL properties of the films deposited under low  $P < 1.5$  Torr and high ( $P > 1.5$  Torr) helium pressures might be connected to a larger porosity of the films deposited at high pressures. A more porous microstructure of these films could enhance the surface area, which was subjected to reactions with ambient air, increasing the role of oxidation in the formation of PL centers. The hypothesis was confirmed by the absence of color interference fringes from the films deposited under the high pressures.

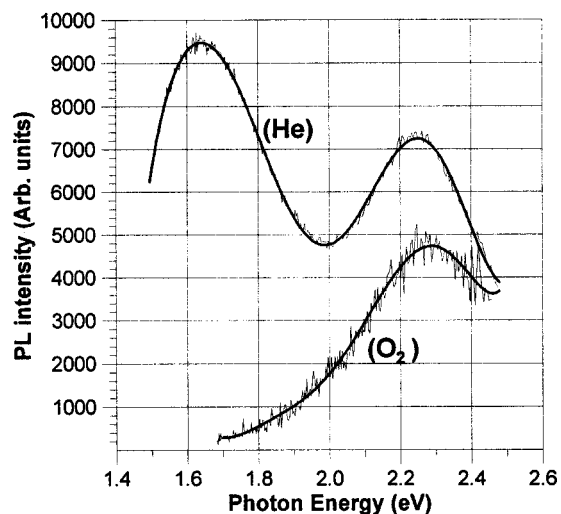


FIG. 5. PL spectra from  $\text{Si/SiO}_x$  films deposited: (He), under 2 Torr of He after 8 weeks of film exposure to humid air; ( $\text{O}_2$ ), under 0.15 Torr of oxygen (the spectrum is multiplied by a factor of 30).

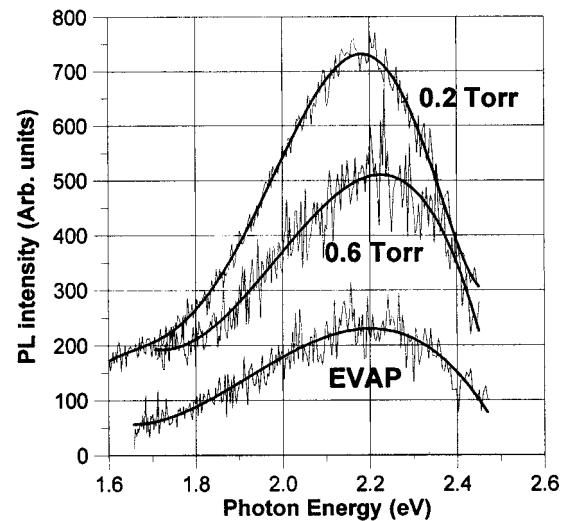


FIG. 6. PL spectra of  $\text{Si/SiO}_x$  films after a thermal annealing in air at  $800^\circ\text{C}$ . Films are deposited by PLA in He at residual pressures of 0.2 and 0.6 Torr, and by a thermal evaporation from a Si target in vacuum (EVAP). The latter two spectra are multiplied by a factor of 5.

However, to verify this, a detailed study of the surface morphology as a function of the residual gas pressure should be carried out. This study is now in progress and will be published elsewhere.

Similar dramatic modification of PL properties was observed after the profound oxidation of the films deposited in helium. It was produced by the annealing of the films in air at  $800^\circ\text{C}$  (10 min). The thermal annealing resulted in the appearance of a single peak around 2.2–2.25 eV for all films prepared under different helium pressures, as shown in Fig. 6. Moreover, the annealing of relatively old samples led to a considerable decrease or even the disappearance of the 1.6–1.7 eV peak. It is interesting to note that the Si-based films, deposited by thermal evaporation from a Si target in vacuum, also exhibited 2.2–2.3 eV PL after the thermal annealing [Fig. 6 (EVAP)], though these films were not photoluminescent just after the fabrication and a prolonged exposition to ambient air. Such a coincidence of PL peak positions gives clear evidence for similar final structures of thermally annealed particles for the films deposited by different methods. It is logical to conclude that these structures are mainly formed during the postdeposition thermal oxidation process.

Similar 2.2–2.3 eV signals were recorded for the laser-ablated films fabricated in an oxygen-containing atmosphere. In particular, this peak was observed for all films deposited under different pressures of pure oxygen as shown in Fig. 5 (spectrum  $\text{O}_2$ ). In contrast to the PLA in helium, the PL signals could be observed immediately after the deposition process, while a prolonged film exposition to air did not result in any detectable increase of the PL intensity. Nevertheless, PL signals from oxygen-deposited films were less intense than that of the He-deposited films by almost an order of magnitude.

#### IV. DISCUSSION

Our studies show that both parameters of laser ablation itself and postdeposition conditions can play a decisive role in the formation of PL properties.

Just after fabrication in a helium inert environment and passivation by the atmospheric air, the films exhibited relatively weak PL signals with a variable peak energy position. The peak position could be tuned from 1.6 to 2.15 eV by a decrease of the helium pressure from 2 Torr to 150 mTorr [Fig. 3(a)]. In our opinion, the generation of pressure-dependent PL signals is not in contradiction with the mechanism of the carrier recombination between quantum confined states in the nanoscale particles.<sup>1</sup> Furthermore, the authors of some previous studies on silicon ablation<sup>12,13,20</sup> reported the nanoparticle size reduction under the helium pressure decrease, which confirms the possibility of the quantum confinement effect. In this case, an air passivation of the nano-clustered film is necessary to saturate dangling bonds, thus reducing nonradiative recombination channels. Nevertheless, other mechanisms may not be ruled out completely.

The naturally and thermally oxidized films, as well as films deposited in oxygen, exhibited quite different PL spectra. In this case we recorded only two PL bands around 1.6–1.7 and 2.2–2.3 eV, whose relative contribution depended on the oxidation method. It should be noted that similar components were observed not only with laser ablated Si-based films,<sup>11–15</sup> but with the films produced by a variety of another techniques as well (see, e.g., Refs. 3–5 and 22–25). The origin of 2.2–2.3 eV PL seems to be relatively clear since it was thoroughly examined in some previous studies of highly oxidized porous silicon<sup>26</sup> and various Si-based films (see, e.g., Refs. 5, 24, and 25). This component was unambiguously attributed to a radiative recombination through defects in SiO<sub>2</sub> structure such as the nonbridging oxygen hole centers.<sup>26,27</sup> The defects are formed in oxygen-related silicon compounds, in particular under the thermal annealing<sup>26</sup> or prolonged film exposure to air.<sup>24</sup> In our experiments the 2.2–2.3 eV component was also recorded after the thermal annealing in air and a prolonged humid oxidation of some films deposited in helium. In addition, this component appeared after a direct deposition of silicon clusters in oxygen-containing atmosphere. We propose that the 2.2–2.3 eV PL centers are effectively formed under a profound oxidation of Si-based films, which was the common feature of these three cases.

A gradual growth of the integral intensity of 1.6–1.7 eV signals with time of the film prolonged exposure to air also gives evidence for a contribution of oxygen in a formation of the PL signals. A similar phenomenon was recorded on films deposited in an oxygen-free atmosphere by a laser decomposition of silane.<sup>3,23</sup> However, there is no common consensus on the origin of these signals in the literature. Taking account the size-independent behavior of the 1.6–1.7 eV signals, some authors attribute it to a recombination through an interfacial layer between the *c*-Si core and the *a*-SiO<sub>2</sub> surface layer.<sup>3,23</sup> On the other hand, some properties of the red components such as a relatively long decay, enable one to ascribe

it to the quantum confinement mechanism (see, e.g., Refs. 5, 22, and 25). In this case the increase of the PL efficiency during the prolonged natural oxidation could be explained by a better dangling bond passivation.

In any case, a clear identification of the PL mechanisms requires further detailed study of mechanical, structural, and PL properties of the deposited and annealed films. These investigations are in progress.

#### V. CONCLUSIONS

Si/SiO<sub>x</sub> nanocrystalline structures have been fabricated by pulsed laser ablation in helium. The as-deposited films exhibit visible PL with peak energy between 1.6 and 2.15 eV. An interaction of silicon nanocrystalline films with oxygen could lead to an appearance and enhancement of fixed peaks around 1.6–1.7 and 2.2–2.3 eV, whose relative contribution depended on the oxidation method.

#### ACKNOWLEDGMENTS

The authors are grateful to M. Charbonneau-Lefort and J.-P. Sylvestre for assistance during the preparation of the experiments and to S. Poulin for the XPS measurements.

Presented at the 47th International AVS Symposium, Boston, MA, 2–6 October 2000.

- <sup>1</sup>L. T. Canham, *Appl. Phys. Lett.* **57**, 1046 (1990).
- <sup>2</sup>H. Takagi, H. Ogawa, Y. Yamazaki, A. Ishizaki, and T. Nakagiri, *Appl. Phys. Lett.* **56**, 2379 (1990).
- <sup>3</sup>Y. Kanemitsu, T. Ogawa, K. Shiraiishi, and K. Takeda, *Phys. Rev. B* **48**, 4883 (1993).
- <sup>4</sup>E. Edelberg, S. Bergh, R. Naone, M. Hall, and B. S. Aydil, *Appl. Phys. Lett.* **68**, 1415 (1996).
- <sup>5</sup>K. S. Min, K. V. Shcheglov, C. M. Yang, H. A. Atwater, M. L. Brongersma, and A. Polman, *Appl. Phys. Lett.* **69**, 2033 (1996).
- <sup>6</sup>L. A. Chiu, A. A. Seraphin, and K. D. Kolenbrander, *J. Electron. Mater.* **23**, 347 (1994).
- <sup>7</sup>I. A. Movtchan, W. Marine, R. W. Dreyfus, U. C. Lee, M. Sentis, and M. Autric, *Appl. Surf. Sci.* **96–98**, 251 (1996).
- <sup>8</sup>D. B. Geohegan, A. A. Puzos, G. Duscher, and S. J. Pennycook, *Appl. Phys. Lett.* **72**, 2987 (1998).
- <sup>9</sup>D. B. Geohegan, A. A. Puzos, G. Duscher, and S. J. Pennycook, *Appl. Phys. Lett.* **73**, 438 (1998).
- <sup>10</sup>E. Werwa, A. A. Seraphin, L. A. Chiu, C. Zhou, and K. D. Kolenbrander, *Appl. Phys. Lett.* **64**, 1821 (1994).
- <sup>11</sup>I. A. Movtchan, R. W. Dreyfus, W. Marine, M. Sentis, M. Autric, G. Le Lay, and N. Merk, *Thin Solid Films* **255**, 286 (1995).
- <sup>12</sup>Y. Yamada, T. Orii, I. Umezu, Sh. Takeyama, and T. Yoshida, *Jpn. J. Appl. Phys., Part 1* **35**, 1361 (1996).
- <sup>13</sup>T. Makimura, Y. Kunii, and K. Murakami, *Jpn. J. Appl. Phys., Part 1* **35**, 4780 (1996).
- <sup>14</sup>T. Makimura, Y. Kunii, N. Ono, and K. Murakami, *Appl. Surf. Sci.* **127–129**, 388 (1998).
- <sup>15</sup>I. Umezu, K. Shibata, S. Yamaguchi, A. Sugimura, Y. Yamada, and T. Yoshida, *J. Appl. Phys.* **84**, 6448 (1998).
- <sup>16</sup>L. Patrone, D. Nelson, V. I. Safarov, M. Sentis, W. Marine, and S. Giorgio, *J. Appl. Phys.* **87**, 3829 (2000).
- <sup>17</sup>A. V. Kabashin, M. Charbonneau-Lefort, M. Meunier, and R. Leonelli, *Appl. Surf. Sci.* **168**, 328 (2000).
- <sup>18</sup>B. D. Cullity, *Elements of X-ray Diffraction* (Addison-Wesley, Reading, MA, 1978).
- <sup>19</sup>E. Bardet, J. E. Bouree, M. Cuniot, J. Dixmier, P. Elkaim, J. Le Duigou, A. R. Middy, and J. Perrin, *J. Non-Cryst. Solids* **198–200**, 867 (1996).
- <sup>20</sup>D. H. Lowndes, C. M. Rouleau, T. Thundat, G. Duscher, E. A. Kenik, and S. J. Pennycook, *Appl. Surf. Sci.* **127–129**, 355 (1998).

- <sup>21</sup>S. Hayashi, S. Tanimoto, and K. Yamamoto, *J. Appl. Phys.* **68**, 5300 (1990).
- <sup>22</sup>S. Li, S. J. Silvers, and M. S. El-Shall, *J. Phys. Chem. B* **101**, 1794 (1997).
- <sup>23</sup>S. Botti, R. Coppola, F. Gourbilleau, and R. Rizk, *J. Appl. Phys.* **88**, 3396 (2000).
- <sup>24</sup>H. Tamura, M. Ruckschloss, T. Wirschem, and S. Veptek, *Appl. Phys. Lett.* **65**, 1537 (1994).
- <sup>25</sup>A. J. Kenyon, P. F. Trwoga, C. W. Pitt, and G. Rehm, *J. Appl. Phys.* **79**, 9291 (1996).
- <sup>26</sup>S. M. Prokes, *Appl. Phys. Lett.* **62**, 3244 (1993).
- <sup>27</sup>S. Munekuni, T. Yamanaka, Y. Shimogaichi, K. Nagasawa, and Y. Hama, *J. Appl. Phys.* **68**, 1212 (1990).